Acta Crystallographica Section D
Biological Crystallography
ISSN 0907-4449

Structures of monomeric, dimeric and trimeric PCNA: PCNA-ring assembly and opening

Vladena Hlinkova,[a]‡ Guangxin Xing,[a] Jacob Bauer,[a]‡ Yoon Jung Shin,[a] Isabelle Dionne,[b] Kanagalaghatta R. Rajashankar,[c] Stephen D. Bell[b]§ and Hong Ling[a]*

[a]Department of Biochemistry, University of Western Ontario, London, Ontario N6A 5C1, Canada, [b]The Medical Research Council Cancer Cell Unit, Hutchison MRC Centre, Hills Road, Cambridge CB2 2XZ, England, and [c]NE-CAT, Advanced Photon Source, Argonne National Laboratory, 9700 South Cass Avenue, Argonne, IL 60439, USA

‡ Current address: Institute of Molecular Biology, Slovak Academy of Sciences, Dúbravská cesta 21, 845 51 Bratislava, Slovak Republic.
§ Current address: Sir William Dunn School of Pathology, South Parks Road, Oxford OX2 6NA, England.

Correspondence e-mail: hling4@uwo.ca

Received 4 June 2008
Accepted 11 July 2008

PDB References: PCNA3, 2ijx, r2ijxsf; PCNA1–PCNA2, 2io4, r2io4sf; PCNA1–PCNA2–PCNA3, 2nti, r2ntisf.

DNA sliding clamps form an oligomeric ring encircling DNA and serve as a moving platform for DNA-processing proteins. The opening and closing of a sliding-clamp ring is essential to load the clamp onto DNA in order to perform its functions. The molecular details of how clamp rings open and enclose DNA are still not clear. Three PCNA homologues have been found in *Sulfolobus solfataricus* which form a heterotrimer. Taking advantage of their hetero-oligomeric nature, the structures of the PCNAs in monomeric PCNA3, dimeric PCNA1–PCNA2 and trimeric PCNA1–PCNA2–PCNA3 forms were determined at resolutions of 2.6–1.9 Å. The distinct oligomeric structures represent different stages in ring formation, which were verified in solution by ultracentrifugation analysis. The heterodimer opens in a V-shape of 130°, while the heterotrimers form a ring with a 120° rotation between monomers. The association of a rigid PCNA3 monomer with an opened PCNA1–PCNA2 heterodimer closes the ring and introduces a spring tension in the PCNA1–PCNA2 interface, thus bending the nine-stranded intermolecular β-sheet to fit the 120° rotation. The release of the spring tension as PCNA3 dissociates from the ring may facilitate ring opening. The structural features in different assemblies present a molecular model for clamp ring assembly and opening.

1. Introduction

DNA-replication sliding clamps are essential in DNA replication and repair and are present in eukaryotes, prokaryotes and archaea (Lee & Alani, 2006; Warbrick, 2000; Tsurimoto, 1999; Hingorani & O'Donnell, 2000; Kelman, 1997; Umar *et al.*, 1996). The sliding-clamp protein is a six-domain ring that encircles DNA and initially functions as a processivity factor for replicative DNA polymerases (Kong *et al.*, 1992; Krishna *et al.*, 1994; Gulbis *et al.*, 1996; Chapados *et al.*, 2004). The eukaryotic and archaeal sliding clamps are homologs of the proliferating cell nuclear antigen (PCNA). Interestingly, while most eucaryotic and archaeal PCNA proteins are homotrimeric rings, three PCNA homologues (PCNA1, PCNA2 and PCNA3) exist in the thermophilic archaeon *Sulfolobus solfataricus* (De Felice *et al.*, 1999; Dionne *et al.*, 2003). Although initial reports claimed that PCNA1 and PCNA3 formed functional homotrimers (De Felice *et al.*, 1999), subsequent work revealed that individually PCNA1, PCNA2 and PCNA3 are monomers and that the functional form of *Sulfolobus* PCNA is a heterotrimer of PCNA1, PCNA2 and PCNA3 (hereafter called PCNA123; Dionne *et al.*, 2003; Roberts *et al.*, 2003; Pascal *et al.*, 2006; Doré *et al.*, 2006; Williams *et al.*, 2006).

Biochemical studies indicated that the heterotrimer assembles in a defined order (Dionne *et al.*, 2003). More specifically, PCNA1 and PCNA2 first form a stable heterodimer (PCNA12) that is then capable of recruiting PCNA3 to complete the ring structure.

Sliding clamps slide along DNA through their positively charged central cavity in the direction of DNA synthesis. PCNA proteins have been found to interact with a wide variety of proteins and are involved in almost every DNA metabolic process, including replication, repair and modification (Maga & Hubscher, 2003; Majka & Burgers, 2004; Lopez de Saro & O'Donnell, 2001; Tsurimoto, 1999). The ring surface facing the primer-extension direction forms a platform that tethers DNA-modifying enzymes (PCNA-interacting proteins; PIPs) on the DNA substrate as the clamps move along the DNA (Waga & Stillman, 1998; Warbrick, 2000). The main PCNA-interacting motif, Q*xx*(M/L/I)*xx*F(Y/W), is well conserved and is called the PIP-box (Warbrick, 2000). Structural studies on PCNA–ligand complexes have shown that the PIP-box binds to the interdomain connecting loop (IDCL) of the sliding clamp and its proximal hydrophobic cavity, which is located on the front face of the ring (Gulbis *et al.*, 1996; Sakurai *et al.*, 2005; Bruning & Shamoo, 2004; Kontopidis *et al.*, 2005). The PCNA123 heterotrimeric ring from *S. solfataricus* has been shown to stimulate the activity of flap endonuclease 1 (Fen1), DNA polymerase B1 (Pol B1) and DNA ligase 1 (Dionne *et al.*, 2003). Fen1, Pol B1 and DNA ligase bind to PCNA1, PCNA2 and PCNA3, respectively, through their PIP-boxes (Dionne *et al.*, 2003). A recently solved structure of PCNA12–Fen1 from *S. solfataricus* reveals that the PIP-box of Fen1 binds to the topologically conserved binding site of PCNA1 (Doré *et al.*, 2006).

The sliding clamps are loaded onto double-strand/single-strand DNA junctions by ATP-driven clamp loaders (Barsky & Venclovas, 2005; Indiani & O'Donnell, 2006; Ellison & Stillman, 2001). During the clamp-loading process, homotrimeric PCNAs, with the help of replication factor C (RFC), are opened at one interface of the ring and adopt a right-handed helix structure matching the right-handed spiral arrangement of RFC (Miyata *et al.*, 2005; Kazmirski *et al.*, 2005). Biochemical studies of the interactions between *Sulfolobus* PCNA subunits revealed that the binding of PCNA3 to the PCNA12 dimer has a K_d that is almost four orders of magnitude higher than that for the binding of PCNA1 to PCNA2 (Dionne *et al.*, 2003). This strongly suggests that one or both of the PCNA1–PCNA3 or PCNA2–PCNA3 interfaces are opened during clamp loading. In support of this, recent studies using covalently fused PCNA subunits have revealed that opening of the PCNA3–PCNA1 interface is both necessary and sufficient for RFC-mediated loading of PCNA onto a DNA substrate (Dionne *et al.*, 2008).

Structural studies of sliding clamps in different assembly intermediates will shed light on the ring opening/closing that is essential for loading onto DNA. In order to better understand the molecular mechanisms of PCNA in DNA loading, we carried out structural analyses of PCNA1, PCNA2 and PCNA3 from *S. solfataricus*. Although two structures of the PCNA heterotrimer have been solved in different space groups (Williams *et al.*, 2006; Pascal *et al.*, 2006), no other free oligomeric form has been reported to take advantage of the hetero-oligomeric system. We present here the crystal structures of the PCNA3 monomer, the PCNA12 heterodimer and the PCNA123 heterotrimer. The structures reveal a rigid PCNA3 monomer, a flexible PCNA12 dimer and a stable PCNA123 trimer. Structural comparison of PCNA in different oligomeric states provides a structural basis for the heterotrimeric ring assembly/opening. The tertiary structures of PCNA1, PCNA2 and PCNA3 also help in interpretation of their distinct binding specificities for their client proteins, such as Fen1, Pol B1 and PolIV.

Table 1
Data-collection and refinement statistics.

Values in parentheses are for the highest resolution shell.

		PCNA12 dimer		
	PCNA3 monomer	Native	SeMet	PCNA123 trimer
Space group	$P4_12_12$	$P2_12_12$	$P2_12_12$	$P2_12_12$
Unit-cell parameters (Å)	$a = b = 85.8$, $c = 264.2$	$a = 105.0$, $b = 112.7$, $c = 101.9$	$a = 105.0$, $b = 112.7$, $c = 101.8$	$a = 148.1$, $b = 222.3$, $c = 80.2$
Wavelength (Å)	1.1000	0.9731	0.9791 (peak)	0.9195
Beamline	NSLS X12B	APS 8BM	APS 8BM	APS 8BM
Resolution range (Å)	30–1.90 (1.92–1.90)	30–2.60 (2.66–2.60)	30–3.30 (3.42–3.30)	30–2.50 (2.59–2.50)
R_{merge}	0.110 (0.490)	0.076 (0.555)	0.093 (0.545)	0.098 (0.625)
Unique reflections	75802	37787	34749	88416
Completeness (%)	96.3 (65.6)	99.9 (99.8)	99.6 (100)	95.4 (93.6)
$I/\sigma(I)$	28.9 (2.2)	8.6 (1.8)	6.6 (2.0)	11.7 (2.0)
Redundancy	23.3 (5.8)	5.1 (5.1)	3.4 (3.4)	8.0 (8.0)
Mosaicity (°)	0.32	0.4	0.66	0.53
Molecules per ASU	4	2	2	3
Structure solution	Molecular replacement	NA	SAD	Molecular replacement
Non-H atoms	8414	7952		18472
Water molecules	544	174		1044
R factor	0.205	0.234		0.211
R_{free} [No. of reflections]	0.251 [1530]	0.260 [1151]		0.250 [1796]
R.m.s.d. bond length (Å)	0.017	0.015		0.011
R.m.s.d. bond angle (°)	1.71	1.57		1.71
Average B factor (Å^2)	42.9	60.8		44.1
Wilson B factor (Å^2)	42.7	74.6		48.6

2. Experimental procedures

2.1. Structure determination and analysis

Protein-sample preparation, crystallization and data collection have been reported previously (Xing *et al.*, 2007). The structure of the SeMet-labeled PCNA12 dimer was

determined at peak wavelength by single anomalous dispersion (SAD) phasing. Selenium sites were located using the program *SHELXD* (Sheldrick, 2008). NCS-averaged density modification and phase extension to a native resolution of 2.6 Å were performed using *DM* (Cowtan & Zhang, 1999). The structures of the PCNA3 monomer and the PCNA123 trimer were solved by molecular replacement with *CNS* (Brünger *et al.*, 1998) and *Phaser* (McCoy *et al.*, 2005) using PCNA from *S. tokodaii* (PDB code 1ud9) and the SAD-phased dimer as search models. Model building was performed with *XtalView* (McRee, 1999), *O* (Jones *et al.*, 1991) and *Coot* (Emsley & Cowtan, 2004). The electron-density maps were improved by NCS averaging and solvent flipping with *CNS* (Brünger *et al.*, 1998). The structures were refined with NCS restraints to 1.9–2.6 Å resolution with *CNS* (Brünger *et al.*, 1998) and *REFMAC*5 (Murshudov *et al.*, 1997). None of the protein residues are in disallowed regions of the Ramachandran plot. The refinement and data-collection statistics are summarized in Table 1. Figures were prepared using *PyMOL* (DeLano, 2002).

2.2. Analytical ultracentrifugation

Sedimentation-equilibrium studies were conducted using a Beckman XL-A analytical ultracentrifuge. An An60Ti rotor and six channel cells with Epon charcoal centerpieces were used. Protein samples were dialyzed against a buffer containing 50 m*M* Tris–HCl pH 7.5 and 100 m*M* NaCl. Centrifugation was carried out at 293 K. PCNA subunits were analyzed at three different concentrations in the range 0.2–0.65 mg ml^{-1} and each concentration was sedimented to equilibrium at rotor speeds between 15 000 and 32 000 rev min^{-1}. Data were fitted to a model using single ideal species and analyzed with the Beckman software *Origin* v. 6.0. Buffer density and partial specific volume were calculated from the inferred amino-acid compositions according to Cohn & Edsall (1943).

3. Results

3.1. Structures of PCNAs

The crystal structures of the PCNA3 monomer, PCNA12 dimer and PCNA123 trimer provide crystallographically independent structural information for five copies of PCNA1 and PCNA2 and seven copies of PCNA3. The structures of the PCNAs from *S. solfataricus* are very similar to those of PCNAs from yeast, humans and other archaea (Krishna *et al.*, 1994; Gulbis *et al.*, 1996; Matsumiya *et al.*, 2001). Each PCNA monomer is composed of two topologically similar domains that are linked by an interdomain connecting loop (IDCL; Fig. 1). The three PCNAs are pairwise superimposible upon each other, although the overall sequence identity and the overall sequence similarity are only ∼8–22% among PCNA1, PCNA2 and PCNA3 (Fig. 1*b*). The superposition of the three monomers in the PCNA123 heterotrimer, based on the 200 C$^{\alpha}$ atoms (excluding the loop regions), results in a root-mean-square deviation (r.m.s.d.) of 1.5 Å. PCNA2 and PCNA3 share the same number and type of secondary-structure elements, while PCNA1 has an additional $\beta9'$ strand which is located in the N-terminal domain. The $\beta9'$ strand forms four main-chain hydrogen bonds to $\beta6$ and plays an important role in the unique conformation of the N-terminal part of the PCNA1 IDCL. This part of the PCNA1 IDCL is shifted toward the back face of the ring structure by up to 10 Å compared with the corresponding C$^{\alpha}$ atoms in the IDCLs of PCNA2 or PCNA3. A similar conformation of the PCNA1 IDCL is seen in the presence of the PCNA1 client protein Fen1 (Doré *et al.*, 2006), indicating that binding of a client protein does not significantly perturb the conformation of its docking site on a PCNA monomer. The IDCLs in PCNA2 and PCNA3 are in a similar position to those observed in their previously studied counterparts.

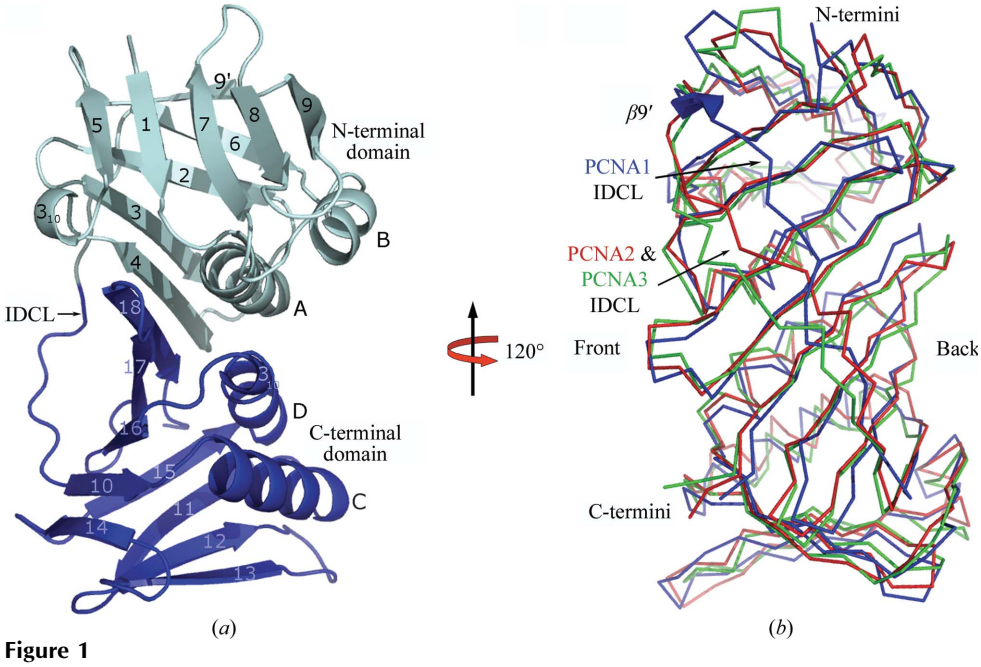

Figure 1
Structures of PCNAs from *S. solfataricus*. (*a*) Ribbon diagram of PCNA1; the secondary structures are named in alphabetical or numeric order for the α-helices and β-strands, respectively, following their order in the primary sequence. (*b*) Superposition of the C$^{\alpha}$ traces of PCNA1 (blue), PCNA2 (red) and PCNA3 (green). The three PCNAs superimpose well with identical secondary-structure elements except for the $\beta9'$ strand in PCNA1. The additional $\beta9'$ strand moves the IDCL in PCNA1 ∼7 Å towards the back face of the ring and is shown as a thick blue arrow.

3.2. Rigid PCNA3 monomers

PCNA3 alone crystallized in space group $P4_12_12$ with four

monomers in the asymmetric unit. The four PCNA3 molecules in the asymmetric unit of the PCNA3 structure randomly pack against each other without forming any physiologically relevant assemblies. The apparent monomeric behavior of PCNA3 in the crystal is in agreement with our ultracentrifugation results (see below) and previous studies (Dionne *et al.*, 2003). Pairwise superposition of these four molecules gave r.m.s.d. values ranging between 0.65 and 1.25 Å over all 244 C^{α} atoms. Smaller r.m.s.d. values (0.50–0.75 Å) were obtained by comparing PCNA3 monomers in the heterotrimers (see below). When the free PCNA3 monomers are compared with PCNA3 in PCNA123 heterotrimers, the r.m.s.d. values are comparable with the differences between the four free PCNA3s. The largest deviations observed in the free PCNA3s are concentrated on the N- and C-terminal end surfaces that form the interfaces contacting the neighboring monomers in the heterotrimer. Therefore, trimer formation seems to reduce the flexibility of PCNA3 at its two ends, but the overall structure of PCNA3 in different oligomeric states remains rigid.

3.3. Opened PCNA12 dimers

The PCNA12 dimer crystallized in space group $P2_12_12$ with two PCNA12 dimers in the asymmetric unit. PCNA1 and PCNA2 form a V-shaped dimer with a 'head-to-tail' assembly, *i.e.* the N-terminal domain of PCNA1 interacts with the C-terminal domain of PCNA2. The two dimers in the asymmetric unit are almost identical and can be superimposed well with an r.m.s.d. of 0.60 Å on all C^{α} atoms. The angle between PCNA1 and PCNA2 in the two V-shaped dimers is 130°, which is 10° larger than the threefold rotation between monomers observed in the trimeric ring (Fig. 2). The two crystallographically independent dimers possess the same open conformation, which indicates that the 130° opening reflects the nature of the dimer and suggests that it is independent of the crystal-packing environment.

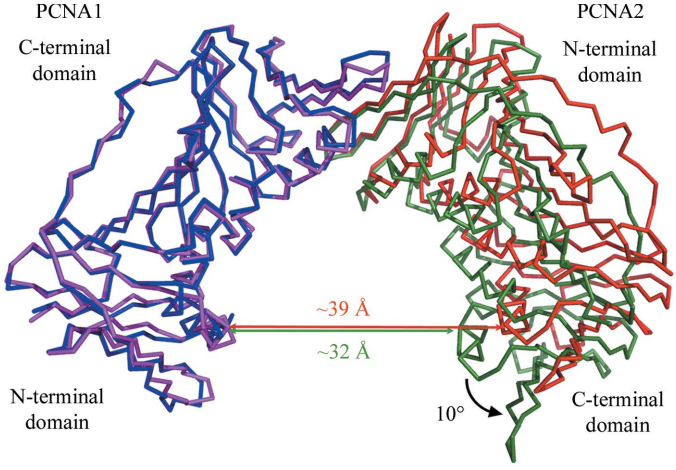

Figure 2
Comparison of the PCNA12 dimer (PCNA1 is blue, PCNA2 is red) with PCNA12 from the heterotrimer (PCNA1, purple; PCNA2, green). The lateral opening in the PCNA12 dimer is about 10° wider than that in PCNA12 from the heterotrimer.

Similar to PCNA3, the PCNA1 and PCNA2 monomers in different oligomeric states are very similar. The r.m.s.d. over all C^{α} atoms between the two PCNA1 molecules and the two PCNA2 molecules in the PCNA12 dimers are 0.53 and 0.57 Å, respectively. Similar r.m.s.d. values (0.46–0.63 Å) were observed among the three copies of the PCNAs in the three trimers in the PCNA123 crystal. The r.m.s.d. values between both PCNA1 and PCNA2 molecules from different oligomeric states range from 0.86 to 1.36 Å. The divergence in the different oligomeric states results from changes in the N-terminal surface of PCNA1 and the C-terminal surface of PCNA2, which are exposed to solvent in the dimers and buried in the interfaces with PCNA3 in the trimers. This strongly suggests that PCNA3 binding only modifies the parts of PCNA1 and PCNA2 which participate in PCNA1–PCNA3 and PCNA2–PCNA3 interface formation.

As PCNA1 and PCNA2 seem to behave as fairly rigid molecules (r.m.s.d. < 1.5 Å), the 10° rotation difference observed between the dimer and trimer must be a rigid-body motion, which leads to a different curvature of the intermolecular nine-stranded β-sheet in PCNA1 and PCNA2. The intermolecular nine-stranded β-sheet of the dimer is less bent than that of the trimer (Fig. 3). The change in bending of the β-sheet results in a 10° lateral opening between PCNA1 and PCNA2 compared with that of PCNA12 in the heterotrimer (Fig. 2). In contrast to the wider lateral opening, 'out-of-plane' movement between the two PCNA molecules is insignificant, with an angular offset of less than 3° from the plane of the ring.

3.4. Ring-shaped PCNA123 trimer

The PCNA123 heterotrimer crystallized in space group $P2_12_12$ with three PCNA123 trimers in the asymmetric unit. The overall assembly is the same as those of the homotrimeric ring structures (Matsumiya *et al.*, 2001; Krishna *et al.*, 1994; Gulbis *et al.*, 1996) and the dimeric β-subunit (Kong *et al.*, 1992), with a pseudo-sixfold symmetry assembled by 'head-to-tail' interactions of N-terminal and C-terminal domains

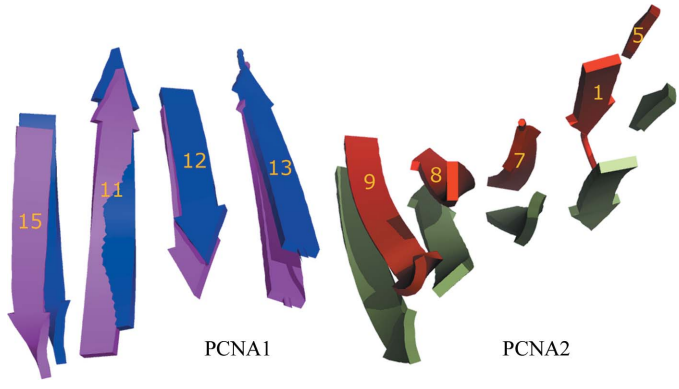

Figure 3
Structural changes in PCNA12 dimers. The different bending of the intermolecular nine-stranded β-sheet at the PCNA1–PCNA2 interface between the PCNA12 dimer (PCNA1, blue; PCNA2, red) and PCNA12 from the heterotrimer (PCNA1, purple; PCNA2, green).

Table 2
Interface parameters of PCNA.

Calculated using the *PISA* server (Krissinel & Henrick, 2005) and the *SC* program (Lawrence & Colman, 1993). The values for the heterotrimers and dimers are averaged over all of the molecules in the asymmetric units. The numbers of hydrogen bonds and salt bridges are listed for the interfaces in the three rings.

Interface	Area (Å^2)	Shape complementarity†	Hydrogen bonds	Salt bridges
PCNA1–PCNA2	1404.0	0.80	12/14/12	8/7/10
PCNA2–PCNA3	1212.4	0.55	7/7/8	3/4/1
PCNA3–PCNA1	1294.4	0.68	11/7/8	1/0/2
PCNA1–PCNA2 (dimer)	1393.0	0.77	9/13	11/8
P. furiosus PCNA	1438.6	0.68	14	14
S. cerevisiae PCNA‡	1317.4	0.61	8	3
Human PCNA	1384.8	0.68	12	1

† Shape complementarity (SC) is in the range 0–1. Interfaces with a SC of 1 match precisely, while interfaces with SC $\simeq$ 0 are uncorrelated in their topography. ‡ Krishna *et al.* (1994).

between PCNA1, PCNA2 and PCNA3 (Fig. 4). The structure of the PCNA123 heterotrimer solved in this study is almost identical to previously reported structures (Pascal *et al.*, 2006; Williams *et al.*, 2006).

PCNA1, PCNA2 and PCNA3 form three unique interfaces in the heterotrimer (Fig. 5). These interfaces differ from each other in amino-acid sequence composition, shape complementarity, charge distribution and number of hydrogen bonds. The PCNA1–PCNA2 interface has the largest buried surface area, 1404 Å^2, and the highest shape complementarity, 0.8, of the three interfaces (Table 2). In addition to hydrophobic interactions, the PCNA1–PCNA2 interface has the most extensive charge–charge and hydrogen-bonding interactions of the three interfaces (Tables 2 and 3). The interface parameters are very similar in the three trimers observed in the asymmetric unit. Very similar interface parameters were obtained for the PCNA1–PCNA2 interface in the dimer structure, suggesting that the strength and unique features of this interface exist independently of PCNA3 binding. The strongest hydrophobic, hydrogen bonding and charge–charge interactions are observed at the PCNA1–PCNA2 interface and this is consistent with previous binding studies showing a K_d of $\sim 10^{-11}$ *M* (Dionne *et al.*, 2003).

Several experimental observations, especially sedimentation-equilibrium analysis (see §3.5), convincingly show that there are no PCNA1, PCNA2 or PCNA3 homotrimers formed in solution. To clarify the absence of homotrimeric rings, we constructed theoretical models of PCNA1–PCNA1, PCNA2–PCNA2 and PCNA3–PCNA3 interfaces while respecting the 'head-to-tail' assembly. The obstacles to homotrimeric ring formation appear to be charge–charge incompatibility of each homotrimeric interface (charge–charge repulsions and close charge–hydrophobic contacts), as well as steric clashes (Fig. 5). The importance of charged interactions in PCNA123 assembly has also been shown by site-directed mutagenesis (Doré *et al.*, 2006).

Similar to all known PCNA homotrimeric rings, the heterotrimer has an overall strong negative charge with the exception of the central channel through which DNA passes

Table 3
Charge interactions at the interfaces.

The interactions were taken from the *PISA* server (Krissinel & Henrick, 2005).

Interface	Interactions	Distance (Å)
PCNA1–PCNA2	Lys175 NZ–Asp75 OD2	3.28
	Lys185 NZ–Asp103 OD1	3.69
	Lys185 NZ–Asp103 OD2	3.37
	Asp149 OD1–Arg82 NE	2.51
	Asp149 OD1–Arg82 NH1	2.74
	Asp149 OD1–Arg108 NH2	3.13
	Asp149 OD2–Arg108 NH1	3.01
	Asp149 OD2–Arg108 NE	3.94
PCNA2–PCNA3	Glu146 OE1–Arg107 NE	3.52
	Glu146 OE2–Arg107 NE	2.99
	Glu146 OE1–Arg107 NH1	3.36
PCNA3–PCNA1	Lys110 NZ–Glu175 OE1	3.70

(Fig. 4). The front face contains the interdomain connecting loops which interact with most of the PCNA-binding proteins (Sakurai *et al.*, 2005; Chapados *et al.*, 2004; Gulbis *et al.*, 1996; Bruning & Shamoo, 2004). In contrast to the homotrimers, the three ligand-binding sites are not identical. The sequences of the interdomain loops and the other loops at the front face are highly divergent, making the topologically equivalent binding sites vary in surface curvature and charge distribution (Fig. 4). The different physicochemical characteristics of the three distinct binding sites presumably account for the observed specificity for the distinct PCNA subunits for different binding

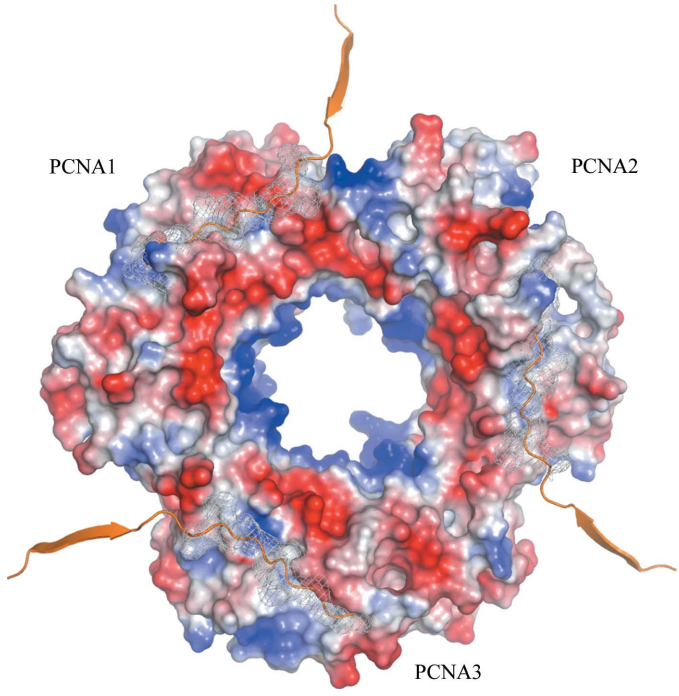

Figure 4
The three distinct ligand-binding sites of the PCNA123 trimer. The front face of the trimeric ring is shown as an electrostatic charged surface with the C-terminal fragment of Pol IV modeled in the three distinct ligand-binding sites. The binding sites are mapped by ribbon-styled C-termini with the side chains as white mesh surfaces. The modeling was performed by superposing the PCNA123 trimer with the β-clamp–PolIV–LF complex (PDB code 1ok7; Bunting *et al.*, 2003).

partners such as Fen1, Pol B1, PolIV and DNA ligase 1 (Dionne *et al.*, 2003, 2008).

3.5. Oligomeric states of the PCNAs in solution

Size-exclusion chromatography has shown distinct peaks corresponding to the individual monomers, PCNA12 dimers and PCNA123 trimers and was used to separate dimers and trimers from each other as well as from monomers (Xing *et al.*, 2007; Dionne *et al.*, 2003). We further studied the oligomeric states of individual PCNA subunits, the PCNA12 dimer and the PCNA123 trimer in solution by using sedimentation equilibrium to determine the molecular weight of each species. The data gave good fits for a single species as determined by the low variance and randomness of the residuals (Fig. 6). The average molecular weights for PCNA1, PCNA2, PCNA3, the PCNA12 dimer and the PCNA123 heterotrimer are in good agreement with their expected theoretical molecular weight

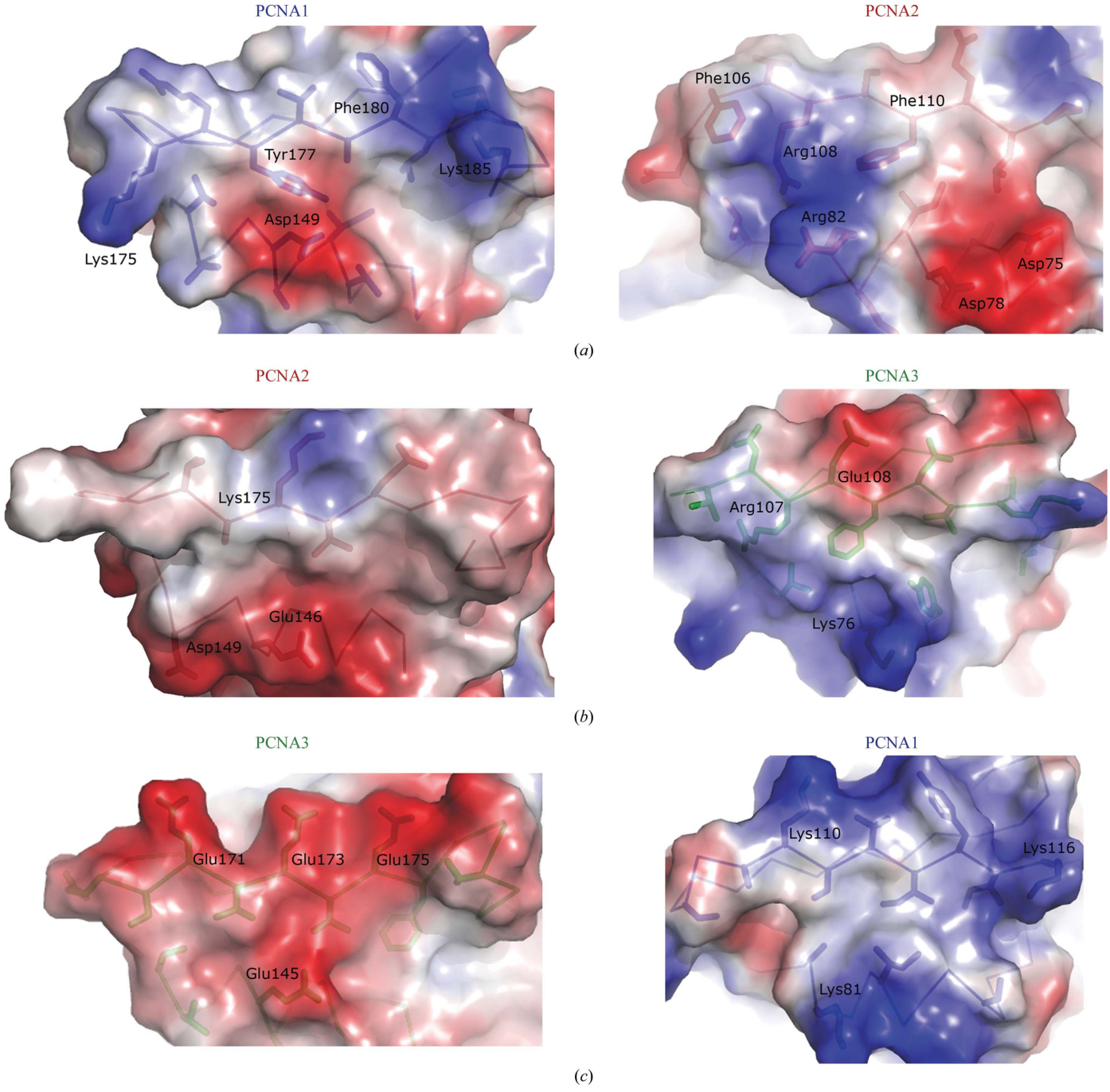

Figure 5
Three sets of interfaces in charged surface representation for the PCNA1–PCNA2 (*a*), PCNA2–PCNA3 (*b*) and PCNA3–PCNA1 (*c*) interfaces. The interfaces on the left are from the C-terminal domains which contact with the N-terminal face on the right. The side chains involved in intermolecular interactions are shown as sticks and charged residues are labeled.

(Table 4). The consistency in molecular weights indicates that the individual PCNAs indeed exist as monomers in solution, while PCNA1 and PCNA2 together form stable dimers and the three different PCNAs together assemble into heterotrimers. The ultracentrifugation analysis verified the structural observations in the crystal structures of monomeric, dimeric and trimeric PCNAs.

Table 4
Molecular weights (MW) determined by sedimentation equilibrium.

Protein	Observed MW (Da)	Theoretical MW (Da)
PCNA1	26200 ± 1500	27535
PCNA2	26100 ± 890	27567
PCNA3	25800 ± 1400	27459
PCNA12	54400 ± 1600	55102
PCNA123	79200 ± 4800	82561

4. Discussion

PCNAs are actively loaded onto the DNA at template-primer junctions by replication factor C (RFC), which is composed of several subunits. An electron-microscopy study of a complex of homotrimeric PCNA and RFC from *Pyrococcus furiosus* on a DNA substrate revealed that the PCNA ring was cracked open with a gap of approximately 5 Å at a single interface (Miyata *et al.*, 2005). Molecular-dynamics simulations have suggested that during loading, homotrimeric PCNAs are opened at one interface and adopt a right-handed helical conformation (Miyata *et al.*, 2005; Kazmirski *et al.*, 2005). This conformation mainly arises from a vertical twisting of the intermolecular nine-stranded antiparallel β-sheet in the homotrimeric ring (Kazmirski *et al.*, 2005). In the present structures of the PCNA12 dimer and the PCNA123 trimer,

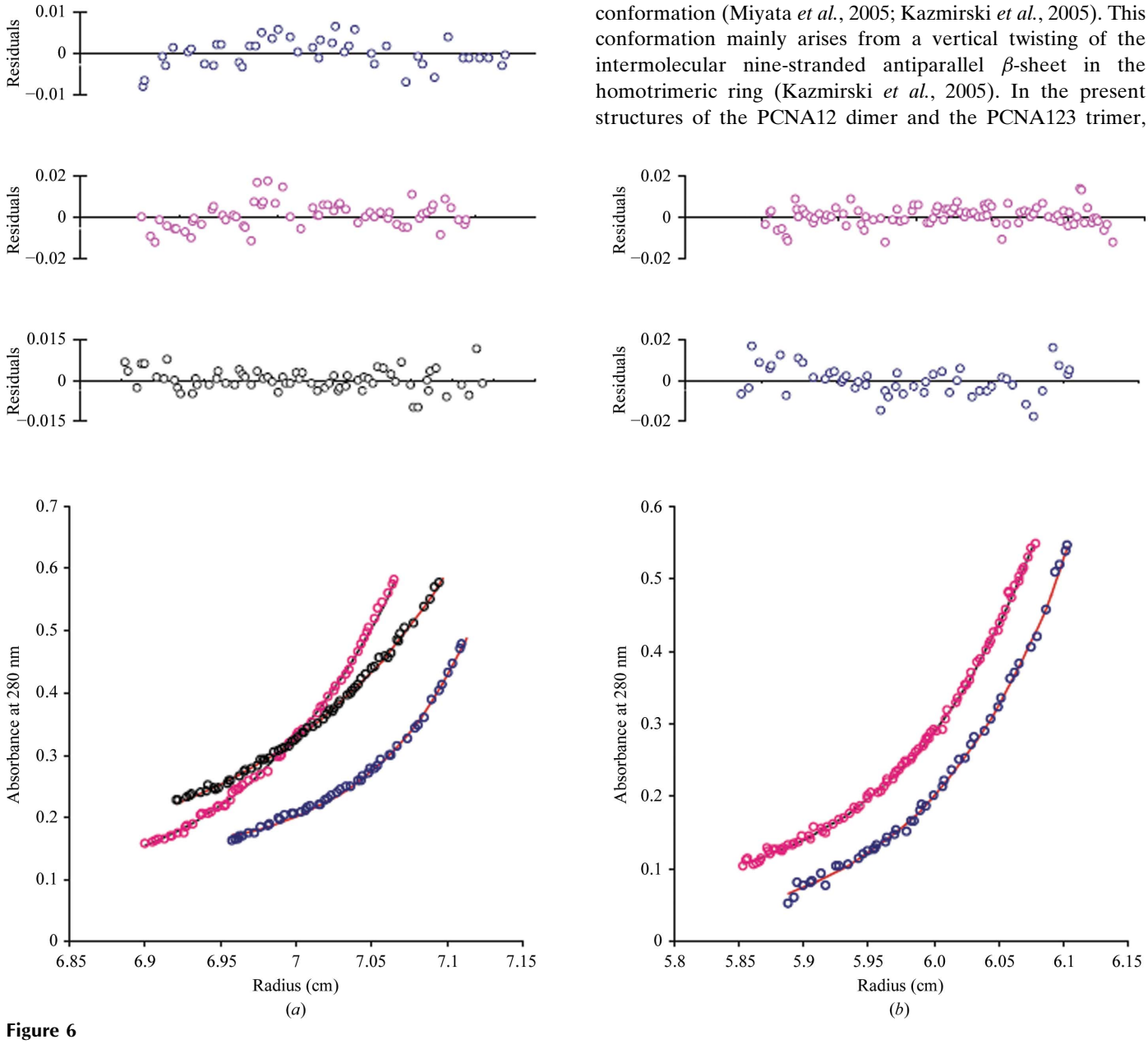

Figure 6
Sedimentation-equilibrium analyses of PCNAs. (*a*) Representative scan of sedimentation-equilibrium data for PCNA1 (blue), PCNA2 (pink) and PCNA3 (black). The average molecular weights for PCNA1, PCNA2 and PCNA3 were determined as 26.2, 26.1 and 25.8 kDa, respectively. (*b*) Representative scan of sedimentation-equilibrium data for the PCNA12 dimer (blue) and PCNA123 trimer (pink). The average molecular weights for the PCNA12 dimer and PCNA123 trimer were determined as 54.4 and 79.2 kDa, respectively.

only the horizontal curvature changes and almost no vertical twist is observed in the corresponding nine-stranded antiparallel β-sheet between the PCNA1 and the PCNA2 molecules. A similar horizontal curvature (a 130° opening) exists in the PCNA12–Fen1 structure (Doré *et al.*, 2006). These observations strongly suggest that the individual subunits of the PCNA123 heterotrimer mainly move in the plane of the ring, which leads to the wider opening seen in the PCNA12 dimer (Figs. 2 and 7).

Recent studies using covalently fused dimers and trimers of *Sulfolobus* PCNA subunits have revealed that opening of only the PCNA3–PCNA1 interface is required for productive loading of PCNA by RFC (Dionne *et al.*, 2008). The PCNA1–PCNA3 interface is the least complementary interface in terms of charge–charge interactions (Fig. 5), although the interface parameters in Table 2 do not show that the PCNA1–PCNA3 interface is the weakest interface. In the PCNA1–PCNA3 interface, the highly negative charged C-terminal surface of PCNA3 is buried by the hydrophobic residues clustered on the PCNA1 N-terminal surface (Fig. 5*c*), which makes the PCNA1–PCNA3 interface less charge–charge compatible than the PCNA2–PCNA3 interface.

Presumably, the complex formed between RFC and PCNA favors opening of the PCNA ring and may supply the additional energy required to facilitate the proposed vertical twisting of the PCNA subunits. The tetramer of RFC small subunits contacts the PCNA12 dimer, while the RFC large subunits contact PCNA3. Previous work has revealed that ATP hydrolysis by the small subunits of RFC is required for release of RFC from PCNA after its loading onto DNA (Seybert & Wigley, 2004). It may be that this reflects conformational alterations within RFC that facilitate the closing of PCNA against the spring tension inherent in the PCNA1–PCNA2 interface. The interaction of all three PCNA subunits with RFC would also prevent dissociation of PCNA3 from PCNA2 upon opening of the PCNA3–PCNA1 interface. Correspondingly, we observe a 130° angle between PCNA1 and PCNA2 in the heterodimer and not the 120° angle found in the heterotrimer. If we model PCNA3 bound to PCNA2 in a PCNA12 heterodimer at a 120° angle, the resulting gap between PCNA1 and PCNA3 is ~6–7 Å wide (Fig. 7*c*). The shortest contacting distance is 5.8 Å, which is between the protruding side chains of Ala109 from PCNA1 and Asp179 from PCNA3. This distance is in good agreement with the ~5 Å distance seen in the RFC–PCNA electron-microscopy structure (Miyata *et al.*, 2005). However, the gap is not wide enough for PCNA to be loaded onto double-stranded DNA. Therefore, it is very likely that additional opening, either further lateral opening or out-of-plane twisting or a combination of both, is provided by RFC. It is also possible that the PCNA ring may be loaded onto single-stranded DNA and then translocated to the template-primer junction as noted by Miyata *et al.* (2005) and Kazmirski *et al.* (2005).

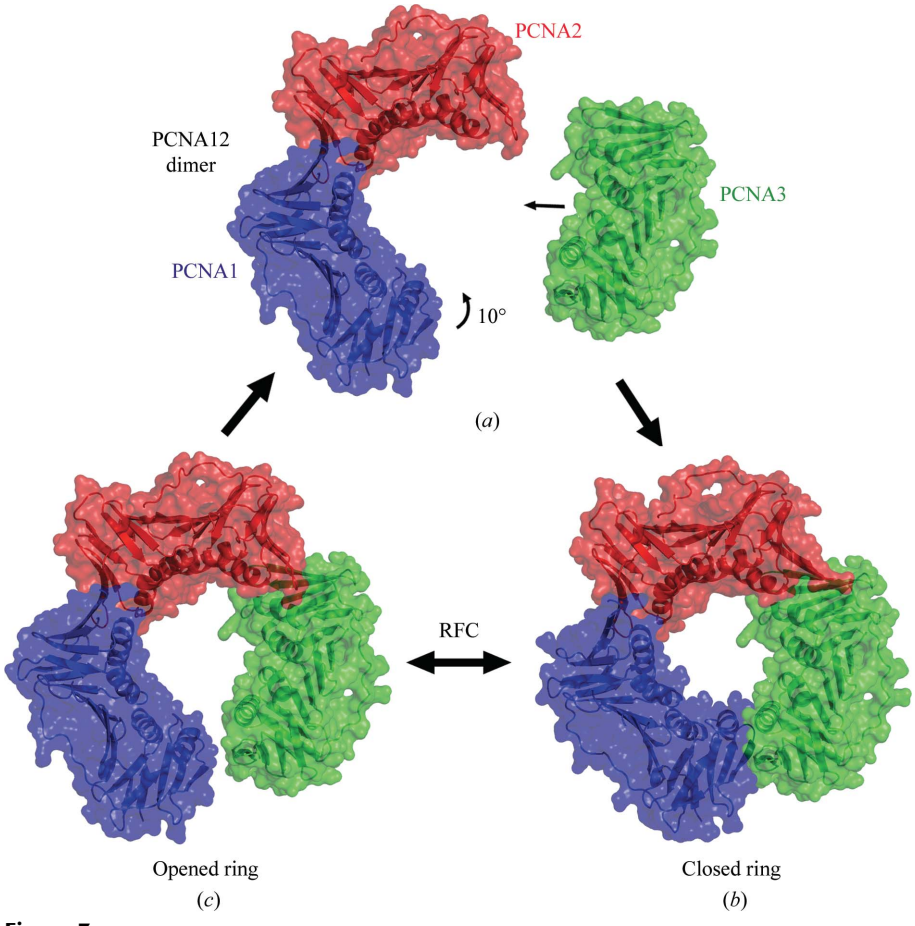

Figure 7
Assembly and opening of the PCNA123 ring. (*a*) PCNA12 dimer and PCNA3 monomer approaching each other during ring assembly. (*b*) The ring of the PCNA123 trimer. (*c*) PCNA12 dimer with PCNA3 modeled in contact with PCNA2 with an angle of 120° as in the trimer. A gap (6–7 Å) remains in the ring-shaped molecule as the angle between PCNA1 and PCNA2 is 130° instead of 120°.

It may appear puzzling that *S. solfataricus*, an archaeon, has a PCNA that is organizationally more complex than that found in eukaryotes. However, in eukaryotes a second sliding clamp in addition to PCNA is found in the form of the 9-1-1 complex (a heterotrimer composed of Rad9–Hus1–Rad1), which participates in cell-cycle control and DNA repair (Kai & Wang, 2003; Parrilla-Castellar *et al.*, 2004; Ellison & Stillman, 2003) and translesion synthesis (Paulovich *et al.*, 1998). Rad9, Rad1 and Hus1 are broadly conserved in eukaryotes (Venclovas & Thelen, 2000; Thelen *et al.*, 1999). A molecular-modeling study proposed that Rad9, Hus1 and Rad1 structurally resemble a PCNA structure and form a heterotrimeric ring with a head-to-tail assembly (Venclovas & Thelen, 2000). The ring structure of

the human 9-1-1 heterotrimeric structure was subsequently observed by electron microscopy (Griffith *et al.*, 2002; Shiomi *et al.*, 2002). Thus, eukaryotic organisms possess two structurally similar ring-like proteins, homotrimeric (PCNA) and heterotrimeric (9-1-1), both of which participate in DNA replication and repair, translesion synthesis (TLS) and control of cell division. For instance, the 9-1-1 complex was found to regulate mutagenic translesion synthesis in *S. cerevisiae* and *S. pombe* (Paulovich *et al.*, 1998; Kai & Wang, 2003; Ellison & Stillman, 2003). It may be that the heterotrimeric PCNA found in *Sulfolobus* represents a predecessor of its eukaryotic sliding-clamp counterparts. The selection for a heterotrimeric PCNA may in part be a consequence of the ability of the distinct PCNA subunits to have specific client proteins. This may facilitate tighter coupling of consecutive transactions on DNA than could be mediated by a homotrimer. In this regard, it may be relevant that *S. solfataricus* grows aerobically at 353 K and thus will be under considerable selective pressure to optimize its DNA damage-repair responses.

This work was supported by Canadian Institutes of Health Research grant MOP-67128 (HL) and funds from the Medical Research Council (SDB). The authors declare no conflict of interest.

References

Barsky, D. & Venclovas, C. (2005). *Curr. Biol.* **15**, R989–R992.

Brünger, A. T., Adams, P. D., Clore, G. M., DeLano, W. L., Gros, P., Grosse-Kunstleve, R. W., Jiang, J.-S., Kuszewski, J., Nilges, M., Pannu, N. S., Read, R. J., Rice, L. M., Simonson, T. & Warren, G. L. (1998). *Acta Cryst.* D**54**, 905–921.

Bruning, J. B. & Shamoo, Y. (2004). *Structure*, **12**, 2209–2219.

Bunting, K. A., Roe, S. M. & Pearl, L. H. (2003). *EMBO J.* **22**, 5883–5892.

Chapados, B. R., Hosfield, D. J., Han, S., Qiu, J., Yelent, B., Shen, B. & Tainer, J. A. (2004). *Cell*, **116**, 39–50.

Cohn, E. J. & Edsall, J. T. (1943). *Proteins, Amino Acids and Peptides*, pp. 157–161. New York: Reinhold.

Cowtan, K. D. & Zhang, K. Y. (1999). *Prog. Biophys. Mol. Biol.* **72**, 245–270.

De Felice, M., Sensen, C. W., Charlebois, R. L., Rossi, M. & Pisani, F. M. (1999). *J. Mol. Biol.* **291**, 47–57.

DeLano, W. L. (2002). *The PyMOL Molecular Graphics System.* http://www.pymol.org.

Dionne, I., Brown, N. J., Woodgate, R. & Bell, S. D. (2008). *Mol. Microbiol.* **68**, 216–222.

Dionne, I., Nookala, R. K., Jackson, S. P., Doherty, A. J. & Bell, S. D. (2003). *Mol. Cell*, **11**, 275–282.

Doré, A. S., Kilkenny, M. L., Jones, S. A., Oliver, A. W., Roe, S. M., Bell, S. D. & Pearl, L. H. (2006). *Nucleic Acids Res.* **34**, 4515–4526.

Ellison, V. & Stillman, B. (2001). *Cell*, **106**, 655–660.

Ellison, V. & Stillman, B. (2003). *PLoS Biol.* **1**, E33.

Emsley, P. & Cowtan, K. (2004). *Acta Cryst.* D**60**, 2126–2132.

Griffith, J. D., Lindsey-Boltz, L. A. & Sancar, A. (2002). *J. Biol. Chem.* **277**, 15233–15236.

Gulbis, J. M., Kelman, Z., Hurwitz, J., O'Donnell, M. & Kuriyan, J. (1996). *Cell*, **87**, 297–306.

Hingorani, M. M. & O'Donnell, M. (2000). *Curr. Biol.* **10**, R25–R29.

Indiani, C. & O'Donnell, M. (2006). *Nature Rev. Mol. Cell Biol.* **7**, 751–761.

Jones, T. A., Zou, J.-Y., Cowan, S. W. & Kjeldgaard, M. (1991). *Acta Cryst.* A**47**, 110–119.

Kai, M. & Wang, T. S. (2003). *Genes Dev.* **17**, 64–76.

Kazmirski, S. L., Zhao, Y., Bowman, G. D., O'Donnell, M. & Kuriyan, J. (2005). *Proc. Natl Acad. Sci. USA*, **102**, 13801–13806.

Kelman, Z. (1997). *Oncogene*, **14**, 629–640.

Kong, X. P., Onrust, R., O'Donnell, M. & Kuriyan, J. (1992). *Cell*, **69**, 425–437.

Kontopidis, G., Wu, S. Y., Zheleva, D. I., Taylor, P., McInnes, C., Lane, D. P., Fischer, P. M. & Walkinshaw, M. D. (2005). *Proc. Natl Acad. Sci. USA*, **102**, 1871–1876.

Krishna, T. S., Kong, X. P., Gary, S., Burgers, P. M. & Kuriyan, J. (1994). *Cell*, **79**, 1233–1243.

Krissinel, E. & Henrick, K. (2005). *CompLife 2005*, edited by R. B. Michael, G. Robert, K. Diederichs, O. Kohlbacher & I. Fischer, pp. 163–174. Berlin/Heidelberg: Springer.

Lawrence, M. C. & Colman, P. M. (1993). *J. Mol. Biol.* **234**, 946–950.

Lee, S. D. & Alani, E. (2006). *J. Mol. Biol.* **355**, 175–184.

Lopez de Saro, F. J. & O'Donnell, M. (2001). *Proc. Natl Acad. Sci. USA*, **98**, 8376–8380.

McCoy, A. J., Grosse-Kunstleve, R. W., Storoni, L. C. & Read, R. J. (2005). *Acta Cryst.* D**61**, 458–464.

McRee, D. E. (1999). *J. Struct. Biol.* **125**, 156–165.

Maga, G. & Hubscher, U. (2003). *J. Cell Sci.* **116**, 3051–3060.

Majka, J. & Burgers, P. M. (2004). *Prog. Nucleic Acid Res. Mol. Biol.* **78**, 227–260.

Matsumiya, S., Ishino, Y. & Morikawa, K. (2001). *Protein Sci.* **10**, 17–23.

Miyata, T., Suzuki, H., Oyama, T., Mayanagi, K., Ishino, Y. & Morikawa, K. (2005). *Proc. Natl Acad. Sci. USA*, **102**, 13795–13800.

Murshudov, G. N., Vagin, A. A. & Dodson, E. J. (1997). *Acta Cryst.* D**53**, 240–255.

Parrilla-Castellar, E. R., Arlander, S. J. & Karnitz, L. (2004). *DNA Repair (Amst.)*, **3**, 1009–1014.

Pascal, J. M., Tsodikov, O. V., Hura, G. L., Song, W., Cotner, E. A., Classen, S., Tomkinson, A. E., Tainer, J. A. & Ellenberger, T. (2006). *Mol. Cell*, **24**, 279–291.

Paulovich, A. G., Armour, C. D. & Hartwell, L. H. (1998). *Genetics*, **150**, 75–93.

Roberts, J. A., Bell, S. D. & White, M. F. (2003). *Mol. Microbiol.* **48**, 361–371.

Sakurai, S., Kitano, K., Yamaguchi, H., Hamada, K., Okada, K., Fukuda, K., Uchida, M., Ohtsuka, E., Morioka, H. & Hakoshima, T. (2005). *EMBO J.* **24**, 683–693.

Seybert, A. & Wigley, D. B. (2004). *EMBO J.* **23**, 1360–1371.

Sheldrick, G. M. (2008). *Acta Cryst.* A**64**, 112–122.

Shiomi, Y., Shinozaki, A., Nakada, D., Sugimoto, K., Usukura, J., Obuse, C. & Tsurimoto, T. (2002). *Genes Cells*, **7**, 861–868.

Thelen, M. P., Venclovas, C. & Fidelis, K. (1999). *Cell*, **96**, 769–770.

Tsurimoto, T. (1999). *Front. Biosci.* **4**, D849–D858.

Umar, A., Buermeyer, A. B., Simon, J. A., Thomas, D. C., Clark, A. B., Liskay, R. M. & Kunkel, T. A. (1996). *Cell*, **87**, 65–73.

Venclovas, C. & Thelen, M. P. (2000). *Nucleic Acids Res.* **28**, 2481–2493.

Waga, S. & Stillman, B. (1998). *Annu. Rev. Biochem.* **67**, 721–751.

Warbrick, E. (2000). *Bioessays*, **22**, 997–1006.

Williams, G. J., Johnson, K., Rudolf, J., McMahon, S. A., Carter, L., Oke, M., Liu, H., Taylor, G. L., White, M. F. & Naismith, J. H. (2006). *Acta Cryst.* F**62**, 944–948.

Xing, G., Hlinkova, V. & Ling, H. (2007). *Cryst. Growth Des.* **7**, 2202–2205.